Current Practice in Neurosciences

Neuro-Oncology: Prediction and Correlation of Histology with Advanced Imaging Techniques

JANUARY 2024

VOLUME 6, ISSUE 1

Ankit Arora[1], Shikha Awasthi[2], Abhilasha Indoria[3], Sabha Ahmed[4], Karthik Kulanthaivelu[5], Sarbesh Tiwari[6]

[1,2,4]Senior Resident, Department of Neuroimaging and Interventional Radiology - NIMHANS, Bengaluru, [3]PhD Candidate, Department of Neuroimaging and Interventional Radiology - NIMHANS, Bengaluru, [5]Associate Professor, Department of Neuroimaging and Interventional Radiology - NIMHANS, Bengaluru, [6]Associate Professor, Department of Diagnostic and Interventional Radiology – AIIMS, Jodhpur, India

Introduction

The field of neuro-oncology deals with primary as well as metastatic tumours of the central nervous system. Though the overall incidence of CNS tumours is low as compared to other organs; their overall mortality and morbidity is quite significant. The primary brain tumours account for approximately 2% of all cancer subtypes in the US with an incidence of approx. 23/100000. Amongst all primary brain tumours, gliomas are the most common and account for about 80% of all malignant brain tumours. Amongst gliomas, glioblastomas are the most common and malignant primary brain tumour with the worst overall survival (1).

With the introduction of 5th edition of WHO classification of CNS tumours 2021, there has been a paradigm shift in diagnosis of CNS tumours based on molecular features combined with histopathological evaluation. Molecular markers were used in addition to histological findings for the first time in 2016. WHO CNS 5th edition builds up on the preceding classification system with addition of specific genetic markers, epigenetic markers e.g., alterations in DNA methylation etc. in addition to immunohistochemistry and histological findings. These changes have drastically changed the practice of neuro-oncology worldwide.

The diagnosis and assessment of treatment response in brain tumour patients is routinely done by using muti-parametric Magnetic resonance imaging (MRI) which includes conventional sequences like T1/T2/FLAIR (Fluid attenuated inversion recovery) along with post gadolinium enhanced images. Advanced sequences like SWI (Susceptibility weighted imaging) /DWI (Diffusion weighted imaging), MR perfusion and MR spectroscopy are also used routinely for diagnosis and follow up.

In addition to the qualitative and semi-quantitative data visible to the radiologists, the MR images also contain a massive amount of interpretable quantitative information which may not be visible to the naked eye; however, can be assessed by latest computational methods (2). This is an emerging field known as Radiomics which involves extraction of high throughput quantifiable data from available radiologic images. Machine learning methods are used to extract this data which further creates multiple mineable databases that can be used for diagnosis and further characterization of CNS tumours. In addition, this data can also be used to identify and predict genetic alterations. This combined study of data from radiology and genetics is known as radiogenomics.

In simple terms, radiogenomics involves linking imaging data with genomic data. The radiogenomic method begins with acquiring genomic material from a fresh frozen paraffin embedded (FFPE) sample or a tissue microarray (TMA) obtained from biopsy specimen of the tumor. Bioinformatics tools, such as sequencing, are then used to discover single or numerous gene alterations. These mutations can be identified using a variety of methods, including immunohistochemistry (IHC) analysis and next-generation sequencing (NGS), such as mRNA sequencing (3). The ultimate objective of radiogenomic studies is to identify direct relationships between gene mutations, pathways, and distinguished imaging phenotypes. Additionally, these studies aim to identify particular target mutations for immunotherapy. For example, multiple radiomics studies have already explored magnetic resonance imaging (MRI) features of GBM, with a primary focus on predicting isocitrate dehydrogenase (IDH) and O6-methylguanine-DNA methyltransferase (MGMT) promoter methylation status, with accurate and promising results. (4) Further, studies have also established the usefulness of radiogenomic in predicting the tumor microenvironment, such as the immune cell infiltration in glioblastomas, which is a direct correlation of overall survival and is an excellent prognostic biomarker. (5) These findings reaffirm that genomics-based biomarkers can be correlated and/or predicted noninvasively by radiomics, allowing for the evaluation of intratumoral genetic heterogeneity; and, if prospectively validated, can be translated to the clinic as a non-invasive, cost-effective genomic test approach, advancing personalised patient care.

In this review article, we will focus on prediction and correlation of histology of common CNS tumours with advanced imaging techniques.

Role of Advanced imaging techniques in neuro-oncology

Diffusion-weighted magnetic resonance imaging (DW-MRI) serves as a pivotal tool for characterizing tissues based on variations in proton movement freedom. Notably,

the apparent diffusion coefficient (ADC), derived from DW-MRI, has demonstrated a significant association with tumor cellularity or density. Recent advancements, such as high b-value DW-MRI (utilizing b-values >3000 s/mm^2), surpass conventional methods in distinguishing tumor tissue from normal brain parenchyma. Techniques like diffusion kurtosis imaging (DKI), histogram curve-fitting, functional diffusion map (fDM), and restriction spectrum imaging (RSI) further refine DW-MRI data, offering enhanced imaging markers and improved tumor detection specificity by isolating tumor cell diffusion properties from extracellular processes like edema.

Perfusion-weighted magnetic resonance imaging (PW-MRI) techniques play a crucial role in assessing tissue blood flow, detecting pathological alterations in tissue vascularity characteristic of brain tumors. Dynamic susceptibility contrasts magnetic resonance imaging (DSC-MRI) and dynamic contrast-enhanced magnetic resonance imaging (DCE-MRI) quantify paramagnetic contrast agent bolus and vascular permeability, respectively. While DSC-MRI is commonly used in clinical settings, DCE-MRI boasts superior signal-to-noise ratio and spatial resolution, albeit with longer acquisition times. Standardizing imaging acquisition parameters and postprocessing techniques remains pivotal for the clinical application of perfusion imaging. Arterial spin labelling is a relatively recent perfusion method that utilizes endogenously labelled blood water protons as an endogenous diffusible tracer and derives perfusion metrics without the use of any contrast agent.

Magnetic resonance spectroscopy (MRS) provides non-invasive insights into tissue metabolite concentrations. Single-voxel spectroscopy (SVS) and multivoxel spectroscopy (MVS) methods, while valuable in tumor diagnosis and assessment, exhibit operator dependency and reduced sensitivity for lesions <1.5 cm^3. In contrast, 18F-fluorodeoxyglucose (18F-FDG) positron emission tomography (PET) has limited specificity in brain tumor imaging, but newer amino acid PET tracers offer improved lesion-to-background uptake ratios, making them valuable for tumor grading, recurrence detection, and treatment response assessment. Novel PET radiotracer (18) F-fluoromisonidazole (18F-FMISO) aids in visualizing tissue hypoxia.

Radiomics and Radiogenomics

The automated quantitative information extraction from radiological images, known as radiomics, usually takes cues from imperceptible radiographical data. These cues are converted into mineable databases that can be used for a variety of tasks, including diagnosis, prognosis, classification, and assessing or forecasting the effectiveness of particular treatment (6-8).

Genetic mutations often play a role in determining the aggressiveness of tumors, influencing the growth pattern of lesions and their response to treatment. Radiomics extends its reach into the realm of genomics, with radiomic features demonstrating the capacity to identify genetic alterations within tumor DNA and RNA—a concept termed radiogenomics. As genetic mutations dictate tumor aggressiveness and influence response to therapy, the integration of radiomics and genomics presents a powerful approach to unravel the complexities of glioma phenotypes (9,10).

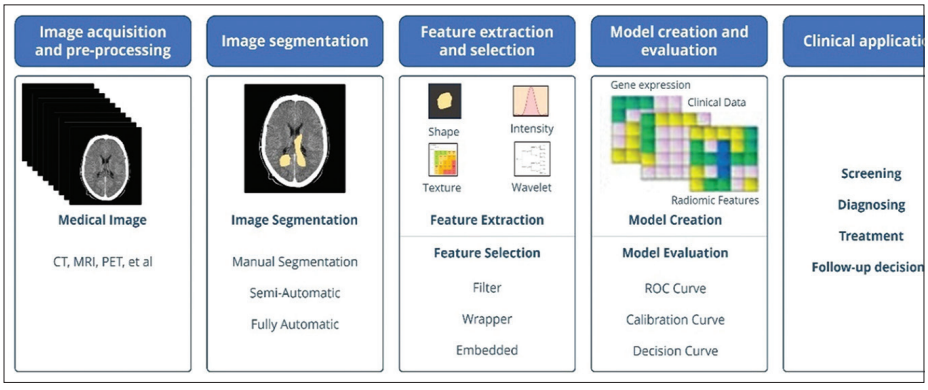

Figure 1: Radiomics workflow

AQ1

Imaging evaluation of specific brain tumors

Adult type diffuse gliomas

Adult type diffuse astrocytoma

In 5th edition of WHO CNS tumours, astrocytoma's are defined as tumours with IDH mutations without 1p/19q codeletion and can have varying grades from 2-4. Most of these tumours also have associated mutations in ATRX and TP53 genes. Homozygous deletion of CDKN2A/B gene is sufficient to assign grade 4 to IDH mutant astrocytoma even without microvascular proliferation or necrosis.

On imaging, IDH mutant gliomas are more often well-circumscribed as compared to IDH wildtype glioma or oligodendroglioma. These tumours also display less frequent enhancement as compared to IDH wildtype tumours. However, minimal enhancement may be seen in grade 3 and 4 tumours [Figure 2] (11).

Younger patients with low grade gliomas or secondary glioblastomas are more likely to have IDH1 mutations, which are generally linked to better outcomes and greater survival rates. The problem of utilizing multimodal MR images to differentiate IDH mutant from IDH wildtype gliomas and connecting imaging features to the mutation has been the subject of numerous investigations. IDH mutations have been reliably identified with high accuracy by computational predictive models using multi-modal MRI in both large and small subject groups, with results ranging from 85% to 97% (12,13).

Earlier techniques focused on single or fewer modalities, such as T2-weighted MRI, FLAIR, or DTI, utilizing features like tumor volume, neoplasm location, T1-CE enhancement, non-enhancing tumor proportion, and FLAIR hyperintensity extent (14,15). These gross features were considered as potential indicators of IDH mutation (16-18). Additionally, the T2-FLAIR mismatch sign, which is suggestive of a 1p/19q non-codeleted astrocytoma with IDH mutation, has been studied. However, its intensity variations across scanning protocols led to decreased agreement among raters and lower sensitivity (with sensitivity at 10.9% and specificity at 100%) (19-21).

Advanced modalities like perfusion-weighted imaging and diffusion MRI have shown promise, with higher relative cerebral blood volume (rCBV) in IDH wildtype cases and lower apparent diffusion coefficient (ADC) values in IDH mutant cases (20,21). Nevertheless, these features may lack sensitivity to the observed variability between patients, making precise and robust biomarker assignment challenging. Rather than relying on a single feature, studies have delved into the extraction of features such as texture and intensity and pooling them into a multivariate framework using radiomics with predictive models. These efforts, especially using The Cancer Imaging Archive dataset (TCIA), have published predictive accuracies between 72-95%, emphasizing the distinctiveness of attributes deduced from contrast enhanced T1 weighted images and FLAIR for identifying IDH mutation (22,12).

Apart from radiomics, deep neural networks, in particular convolutional neural networks (CNNs), have been extensively employed to delineate gliomas with IDH mutation. CNNs, such as ResNET architecture, have shown stability and robustness in discriminating IDH, achieving testing phase accuracies of 85.7%, improved to 89.1%. Data augmentation and transfer learning have been employed to prevent overfitting, contributing to improved generalizability of the classifier (23).

Oligodendroglioma, IDH mutant and 1p/19q-codeleted

Both IDH mutation and presence of 1p/19q codeletion are required for the diagnosis of oligodendroglioma. These tumors may be graded as grade 2 or 3 but they cannot be grade 4. The characteristic imaging findings of oligodendrogliomas include poorly circumscribed margins; internal heterogeneity; presence of internal cysts and calcifications. Heterogeneity is 96% sensitive for oligodendroglioma, whereas calcification was 88% specific for oligodendroglioma [Figure 3] (11). Enhancement may be seen in approx. half of oligodendrogliomas which is usually partial. Ring enhancement and intense enhancement are not usually seen (11,24).

A cortical high-flow sign has recently been identified as increased arterial spin labelling (ASL) signal intensity within tumor-affected cortex compared to normal-appearing cortex

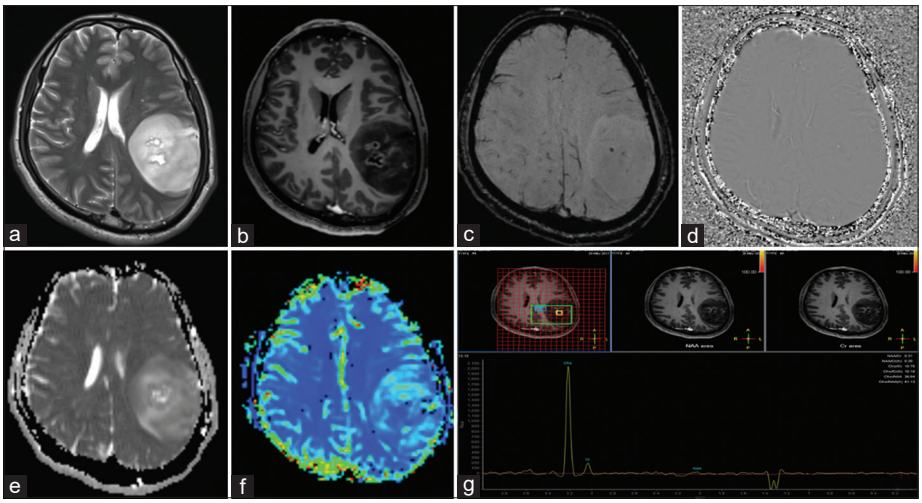

Figure 2: Axial T2 (a) and Postcontrast T1 (b) show a well-defined T2 hyperintense left parietal mass lesion showing internal necrotic components. Small patchy areas of enhancement are seen within rest of the lesion. SWI (c) shows blooming due to microhaemorrhage as confirmed on phase maps (d). Low ADC values are seen (e) with areas of elevated perfusion (f). Multivoxel MRS at 144 TE (g) shows elevated choline and lactate with markedly reduced NAA. Histopathologically found to be anaplastic astrocytoma IDH mutant WHO grade 3

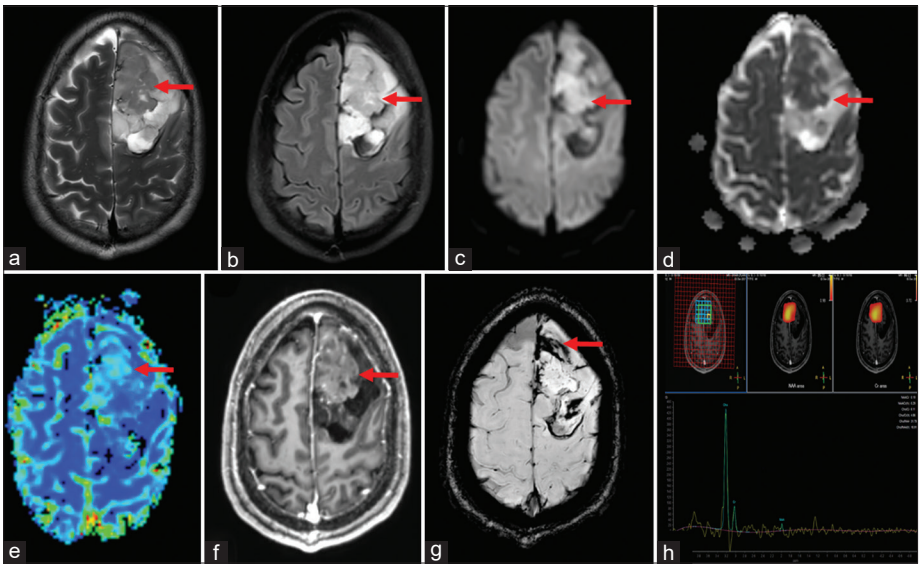

Figure 3: Axial T2 (a) and FLAIR (b) images show gyriform expansile hyperintense solid-cystic mass lesion involving left frontal lobe. DWI Trace (c) and ADC(d) maps show diffusion restriction. Perfusion is moderately elevated in the cortical location on rCBV map (e). There is moderate contrast enhancement seen (f). Extensive blooming is seen on SWI (g). Multivoxel MRS (h) at 144 TE using PRESS technique shows elevated choline with reduced NAA peak. No lactate peak is seen. The tumour was histopathologically confirmed to be oligodendroglioma, NOS, WHO grade 3

in gliomas with IDH mutation and 1p19q codeletion (25). Tumour cells congregate in perivascular spaces or subpial regions of cortical grey matter, which could explain why IDH mutant codeleted gliomas have a higher frequency of the cortical high-flow sign than IDH wild type or IDH mutant noncodeleted gliomas. ASL was also demonstrated to surpass dynamic susceptibility contrast (DSC) in recognising the cortical high-flow sign in oligodendrogliomas in a separate study (25).

Radiomic Features for 1p/19q Prediction

Various radiomic features, including size and shape of tumor, texture, histogram and intensity, have been analysed for predicting 1p/19q status (26). Texture quantifiers demonstrate greater discriminative power compared to other attributes. When compared to textural features, topological features—which quantify geometrical

information or shape and cavities—show better predictive performance, improving accuracy by 5%.

Integration of Age into Radiogenomic Model

The accuracy of predicting 1p/19q status is significantly increased and improved by the use of age into radiogenomic models (27).

Tumor Location's Role in Discrimination

Tumor location plays a vital role in discriminating 1p/19q status (28).

Deep Learning Approach

In deep learning, a recent study utilizing a multi-scale CNN with 30-fold augmented data achieves an accuracy of 87.7% in predicting 1p/19q co-deletion (29).

Glioblastoma

Historically, glioblastomas were defined as diffuse astrocytic tumours which demonstrated evidence of necrosis, increased mitotic activity or microvascular proliferation. However, in 2021 classification; the term glioblastoma is reserved for only IDH wild type tumours. In addition, this term may also be applied to IDH wild type tumours with any of the following: TERT promoter mutation; EGFR amplification or combined gain of Chr 7 and loss of Chr 10. IDH mutant astrocytoma with microvascular proliferation or necrosis are classified as astrocytoma, IDH mutant, CNS WHO grade 4 (30).

On imaging, these tumours demonstrate, T2/FLAIR hyperintensity with areas of restriction of diffusion and blooming on SWI with peripheral, thick and irregular post contrast enhancement. Evidence of raised perfusion is seen in these tumors (31) with raised Cho and reduced NAA with lipid-lactate peak [Figure 4].

MGMT Status Prediction

Methodologies and Accuracies: Radiomics applied to multi-modal MRI (T2, T1-CE, T1, FLAIR) for MGMT status prediction has shown varied accuracies (61-80%) across studies with cohorts ranging from 82 to 193 subjects (32).

Perfusion Imaging: Kickingereder *et al*. incorporated perfusion images, emphasizing higher Gaussian-normalized relative CBV (nrCBV) in contrast enhanced T1weighted images as crucial for MGMT identification (32).

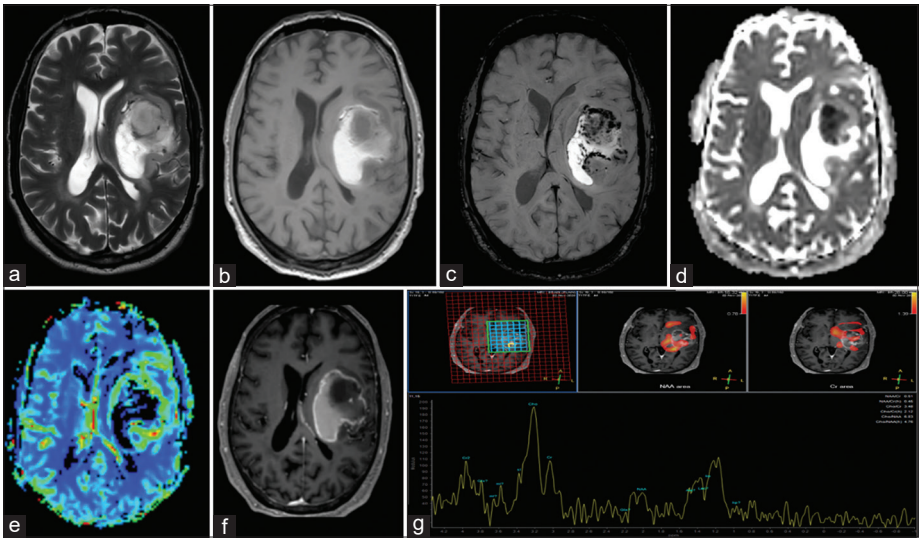

Figure 4: Axial T2 (a) and T1 (b) images show a heterogenous solid cystic mass lesion epicentred in left insula showing intrinsic T1 shortening of the cystic component. There is extensive haemorrhagic residue seen on SWI (c). Focal area of low ADC is seen (d). Peripheral rim of elevated rCBV is noted (e). There is also peripheral rim enhancement seen (f). Multivoxel MRS (g) at 144 TE revealed a choline and lipid peak with reduced NAA. Note the decreased SNR compared to other MRS due to the extensive haemorrhagic products. Histopathologically was confirmed to be Glioblastoma IDH-wild type CNS WHO Grade 4

Deep CNN for Genomic Types: Deep CNNs demonstrated high accuracy in predicting IDH genotype, status of 1p/19q codeletion, as well as methylation of MGMT promotor, revealing distinct imaging features for each genomic type (33,34).

Transcriptomic Delineation of Glioblastomas

Molecular Subtypes: Radiomics-based frameworks successfully delineate the four molecular subtypes namely-classical, proneural, neural and mesenchymal described by Verhaak *et al*. with accuracies ranging from 71% to 76% (35,36).

Paediatric type Diffuse high grade gliomas

This family of tumours includes four subsets of paediatric tumours:

A) Diffuse midline glioma, H3K27 – altered.
B) Diffuse hemispheric glioma, H3G34 – mutant
C) Diffuse paediatric type-high grade glioma, H3-wildtype and IDH -wildtype.
D) Infant-type hemispheric glioma.

Diffuse midline glioma, H3K27-altered

A uniform histopathological feature of these tumours is loss of H3K27me3 which portends a poor prognosis. These tumours are WHO grade 4 tumours. Typically these tumours have a poor overall survival with a median survival duration of approx. 9-11 months (37). The non-invasive prediction of H3K27M mutations stands as a pivotal frontier in the realm of neuro-oncology, offering significant implications for the prognostication of the disease and the exploration of potential targeted therapeutic interventions. These tumors may arise in pons/brainstem as well as in thalami, ganglio-capsular region, cerebellum, cerebellar peduncles, and the spinal cord. The imaging appearance of these tumours is variable. These tumors may exhibit thick enhancing margins or solid enhancement. On the other hand, they may also show more edema, poorly defined margins and more cortical invasion. In an independent study, it was demonstrated that peritumoral ADC values and normalised rCBV values were significant independent predictors of H3K27M mutational status in DMGs [Figure 5] (38).

Multiparametric MRI-based radiomics models demonstrate varying performance across different sequences and machine learning techniques, a recent study, utilizing a combination of all sequences, demonstrated high accuracy (AUC = 0.969) in predicting H3 K27M mutant status in diffuse midline gliomas. The single best performing sequence in predicting the mutant status were T2 weighted images (39).

Diffuse hemispheric glioma- H3G34 mutant

This is a newly described tumour in the 2021 WHO classification and is always graded as grade 4. It is usually seen in the supratentorial brain in older children and young adults. These lesions are hemispheric and may show extension across midline. Most of these tumours

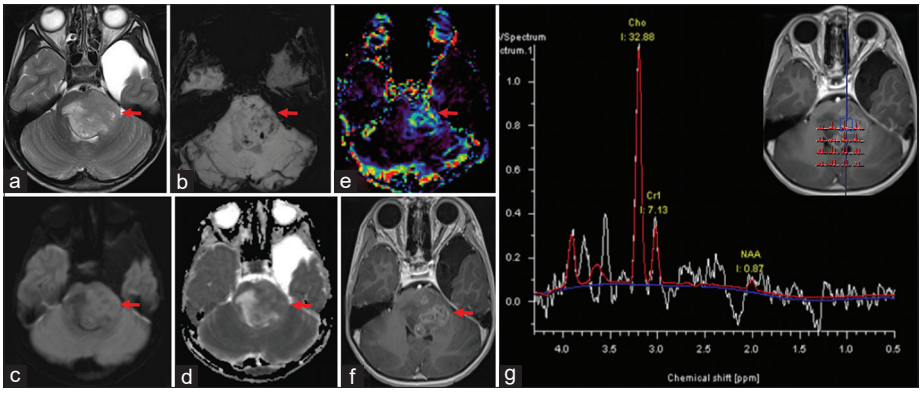

Figure 5: Histopathologically proven case of diffuse midline glioma, H3K27M mutant. Axial T2 weighted demonstrate an expansile heterogeneous signal intensity mass lesion located in the pons. The lesion shows multiple blooming foci on SWI images (b) and demonstrates patchy diffusion restriction as shown in diffusion and corresponding ADC images (c and d). The lesion shows elevated perfusion on r CBV maps (e) and shows heterogenous contrast enhancement (f). MR spectroscopy images reveal (g) elevated choline peak and reduced creatine and NAA peak

are well-defined and expansile with associated necrosis and/or microcalcification (40). Some tumors may show a well-defined mass with an adjacent infiltrative signal. All cases have leptomeningeal contact. Enhancement is variable ranging from none to intense [Figure 6].

Diffuse paediatric-type high grade glioma, H3-wildtype and IDH-wildtype

This is another new tumour entity which was described in the 5th edition of WHO classification. It is an aggressive paediatric tumour which lacks mutations in both IDH and histone 3 genes. On imaging, these tumours resemble adult glioblastomas with high grade features (41).

Infant -type hemispheric glioma

These tumours are aggressive tumours seen in infants. These tumours can show solid, cystic appearance with necrosis and hemorrhage with CSF dissemination. Hence spinal imaging should be done for these tumours.

Paediatric type diffuse low grade gliomas

Four tumour entities are included in this group and are as follows:

A) Angiocentric glioma
B) Diffuse astrocytoma, *MYB- or MYBL1- altered*
C) Polymorphous low grade neuroepithelial tumor of the Young (PLNTY)
D) Diffuse low grade glioma, MAPK Pathway altered.

Angiocentric glioma

This is a rare tumour of children and young adults which is associated with epilepsy. These tend to occur in supratentorial superficial regions. These tumours were recognised as a distinct modality in 2007. On imaging, these tumours have two characteristic features – high intensity on T1WI which appears ribbon like and stalk like T2/FLAIR hyperintensity which extends to the ventricular surface (42). Surgical excision of the tumour usually results in disease free state [Figure 7].

Diffuse astrocytoma, MYB- or MYBL1- altered

This is a newly recognised tumour in the latest WHO classification. This is a highly differentiated tumour and results in seizures, which may be surgically treatable. On imaging, this may present as a well-circumscribed lesion with cysts, T1 hypointensity and T2 hyperintensity. No perilesional edema or post contrast enhancement seen (43).

Polymorphous low-grade neuroepithelial tumour of the young

This is a new tumour entity described in the 2021, WHO classification of the CNS tumours. This is a grade 1 neoplasm and is characterized by aberrant CD34 expression and has a

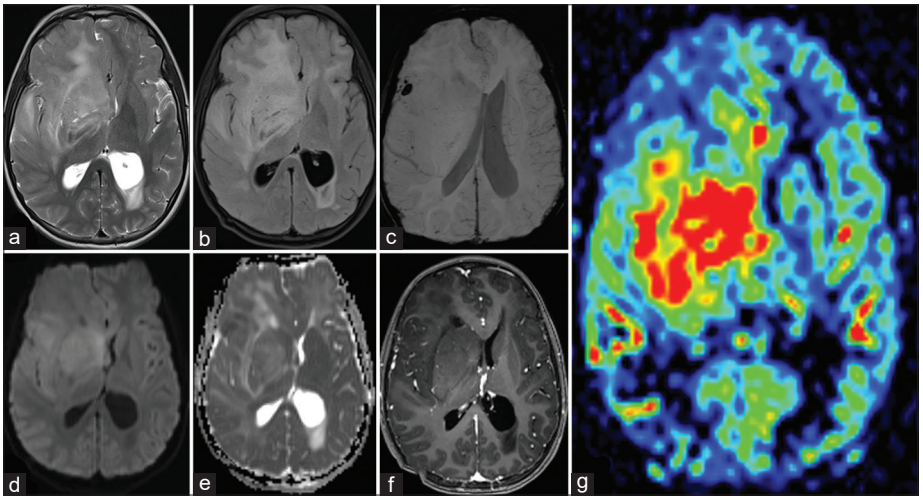

Figure 6: Axial T2 and FLAIR images in a 9-year child reveal a large infiltrative heterogeneously hyperintense mass lesion occupying the right cerebral hemisphere (a and b), few blooming foci are seen in the lesion periphery (c). Axial diffusion images with corresponding ADC maps (d and e) demonstrate patchy diffusion restriction. The lesion does not show significant enhancement (f). Significant elevated perfusion is seen in the right basal ganglia on rCBV maps (g). Final histopathological diagnosis was diffuse hemispheric glioma, H3 G34-mutant, CNS WHO grade 4

distinct DNA methylation signature. On imaging, these tumours are commonly seen in superficial location with temporal predilection. They are commonly well-circumscribed with peripheral cysts, central coarse calcification and show heterogeneous signal (44). These tumours can also show minimal post contrast enhancement [Figure 8].

Diffuse low grade glioma, MAPK Pathway-altered

This is also one of the newly recognised tumours. They are rare tumours and can occur throughout the craniospinal axis. The imaging appearance is heterogeneous, and they may appear similar to pilocytic astrocytoma.

Supratentorial ependymomas

Ependymomas can occur supratentorial as well as infratentorial compartments. The supratentorial tumours behave differently biologically as well as radiologically. Only a

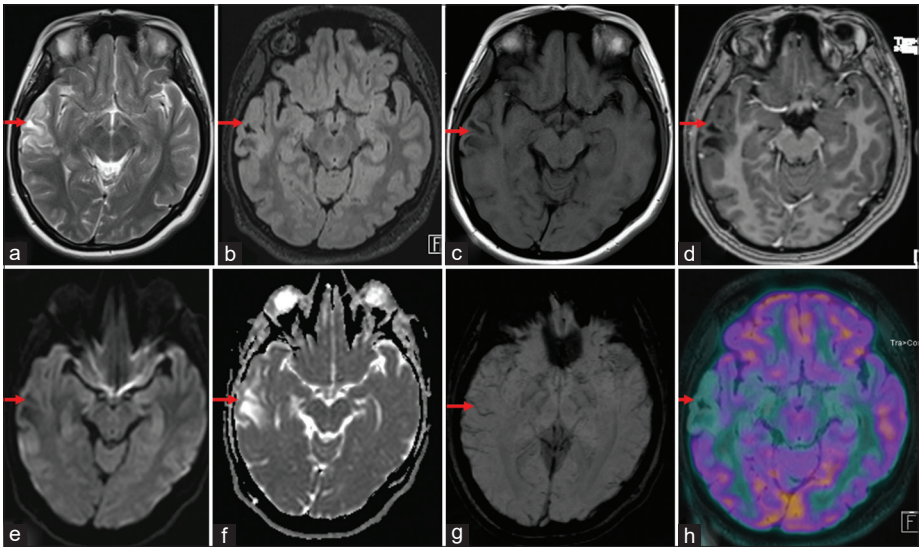

Figure 7: Axial T2 and FLAIR (a and b) images reveal an ill-defined T2 hyperintense and FLAIR inverting lesion noted involving right temporal lobe with accentuation of grey-white matter differentiation. The lesion demonstrated a T1 hyperintense cortical rim and did not show any obvious contrast enhancement (c and d). The lesion demonstrated facilitated diffusion (e and f) and no obvious blooming foci was seen within the lesion (g). FDG PET images (h) reveal hypometabolism in the lesion location. Histopathology was confirmed to be angiocentric glioma

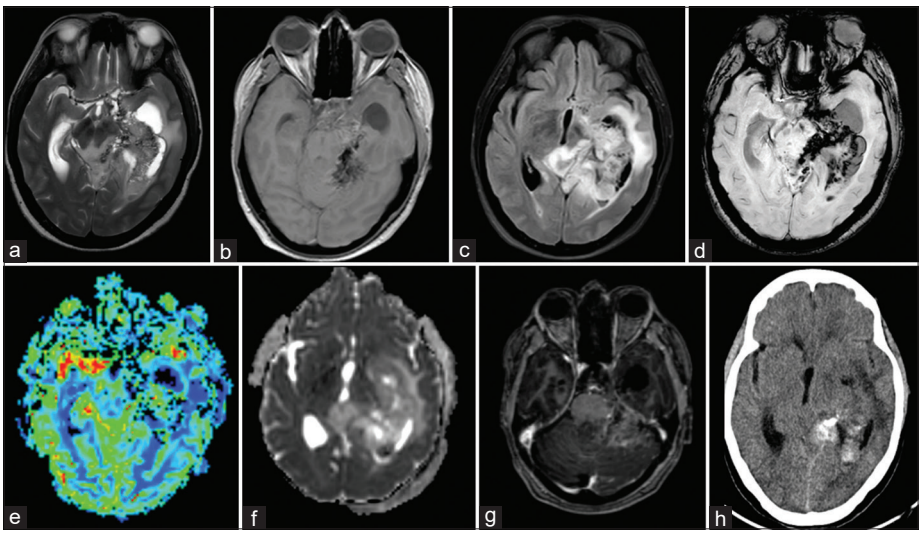

Figure 8: Axial T2 (a), T1 (b), FLAIR (c) shows a diffusely infiltrating mass lesion involving left temporal lobe with extension along perimesencephalic cisterns. There are hypointense areas seen within the lesion showing corresponding blooming on SWI (d) confirmed to calcifications on NCCT (h). Perfusion is not elevated on rCBV map (e). Areas of low ADC are seen (f). Heterogenous ill-defined contrast enhancement is seen (g). Histopathologically it was found to be Polymorphous Low Grade Neuroepithelical Tumour of the Young (PLNTY)

small proportion of these tumours are intraventricular and most of these tumours are high grade. These tumours are further subdivided into: ZFTA fusion positive and YAP1-MAMLD1 fusion. The ZFTA fusion positive tumours are commoner of the two entities and are seen in older children. The common imaging features of these tumours include a large lesion with relatively well-defined margins which has a heterogeneous solid-cystic appearance. Presence of calcification and extension of the lesion to the ventricular surface from pial margin with ADC values approaching those of white matter (45,46) Machine learning-based diagnostic model has been investigated to distinguishing adult supratentorial extraventricular ependymoma (STEE) from high-grade gliomas (HGG). FLAIR-derived features have demonstrated high classification performance for all tumor groups, and texture-based radiomic features from FLAIR were crucial in discriminating STEE from HGG (47).

Medulloblastoma

The four molecular subtypes of medulloblastoma (MB) defined in the 2021 WHO classification are:

A) MB, WNT activated
B) MB, SHH-activated and TP53 wildtype
C) MB, SHH-activated and TP-53 mutant
D) MB, non-WNT/non-SHH.

Wingless (WNT) tumors are the rarest subtype; but they confer the best prognosis. On the other hand, group 3 tumours have the worst prognosis. On conventional imaging, SHH tumours are more homogenous than WNT tumours on T1WI. WNT tumours show more heterogenous post contrast enhancement than SHH tumours (48). WNT tumours are primarily located in CP angle location. Cerebellar peripheral location is primarily seen in SHH tumours [Figure 10]. Non WNT/non-SHH (erstwhile group 3 and group 4) show poor enhancement and spinal metastasis (48).

The radiogenomics exploration of pediatric medulloblastoma (MB) serves as a crucial avenue for improving risk stratification in this malignancy, offering valuable insights that can inform therapeutic decisions, facilitate family counselling, and guide the selection of patient cohorts suitable for targeted genetic analysis. In a retrospective study by Zhang *et al* (49) spanning 12 international pediatric sites from July 1997 to

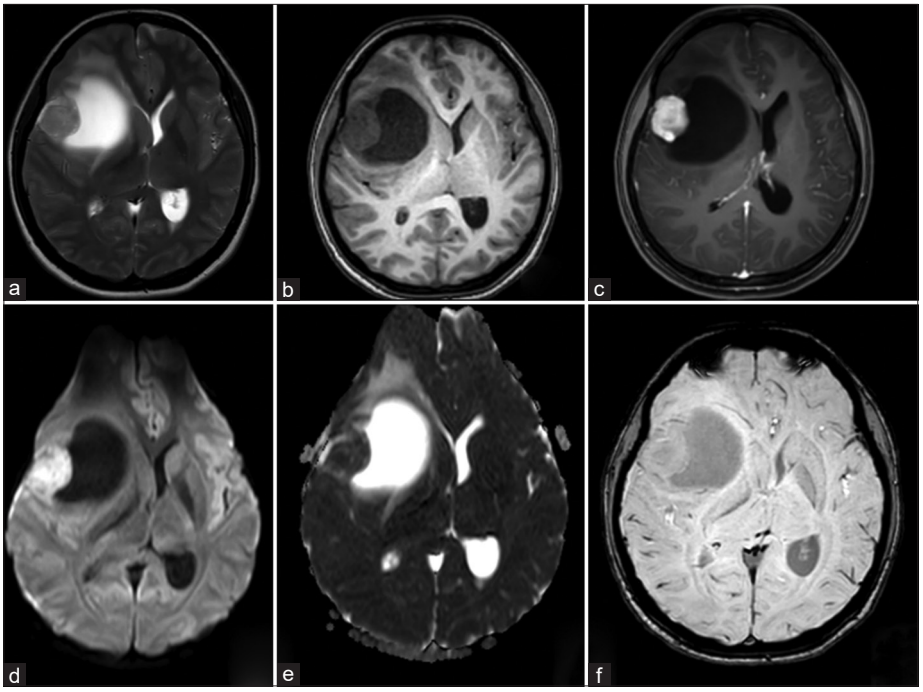

Figure 9: In a 23-year-old lady, there is a cyst with solid mural nodule seen in right supratentorial compartment with the solid component appearing T2 hyperintense (a), T1 hypointense (b) with avid enhancement (c), diffusion restriction on trace (d) and ADC maps (e). There is no blooming on SWI (f). The lesion was found to be ependymoma WHO grade 3 with L1CAM positivity

AQ1

May 2020, the researchers engaged in a comprehensive analysis of MRI scans from newly diagnosed pediatric MB cases. Extracting 1800 features from T2- and contrast-enhanced T1-weighted preoperative MRI scans, they devised a sophisticated two-stage sequential classifier. This classifier first discerns non-wingless (WNT) and non-sonic hedgehog (SHH) MB, followed by a differentiation between therapeutically relevant WNT and SHH subgroups. Additionally, a classifier was developed to distinguish high-risk group 3 from group 4 MB. The study, encompassing 263 patients, demonstrated that the two-stage classifier outperformed a single-stage multiclass classifier. The combined, sequential classifier achieved impressive microaveraged F1 and binary F1 scores, particularly for WNT. The classifier distinguishing group 3 from group 4 MB displayed a remarkable performance, further validating the efficacy of the machine learning approach.

Embryonal tumours with multilayered rosettes (ETMR)

These are WHO grade 4, rare, small round blue cell tumours. They belong to one of the most aggressive tumours seen in children <4 years. These tumours are more common in girls, unlike the other CNS embryonal tumours. Amplification of C19MC region on chromosome 19 is identified as characteristic feature of these tumours. On imaging, these tumours are seen as large lesions with minimal or absent perilesional edema. They show minimal or weak enhancement with intratumoral macrovessels. Calcification may be commonly seen. These tumours show restricted diffusion with low ADC (50).

Pilocytic astrocytomas

Pilocytic astrocytomas (PA) belong to the circumscribed astrocytic gliomas and are seen in children and young adults. Majority of sporadic PA in children are seen in the cerebellum. When seen in patients with NF1, they commonly involve optic pathway or hypothalamus. In adults, they are commonly supratentorial (51,52) On conventional imaging, PA may appear as a cystic lesion with enhancing mural nodule, completely solid or heterogenous with mixed solid-cystic appearance. In pilocytic astrocytoma, a distinctive characteristic of the enhancing nodules is their tendency to exhibit facilitated diffusion while concurrently demonstrating low perfusion on imaging studies.

Conclusion

In conclusion, this review underscores the multifaceted role of advanced imaging techniques in neuro-oncology, emphasizing their diagnostic, predictive, and prognostic significance. As technology advances and our understanding of the molecular underpinnings of brain tumors deepens, the integration of advanced imaging with histological and genomic insights promises to usher in a new era of precision medicine in the management of these complex and challenging conditions.

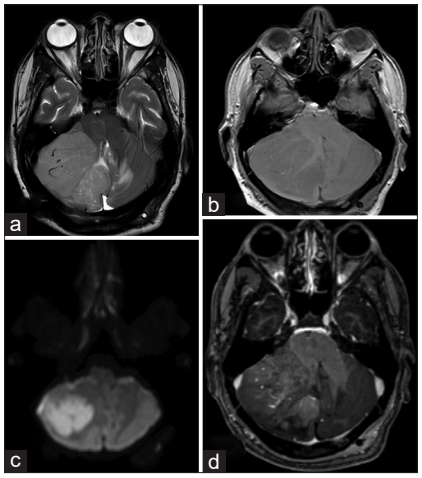

Figure 10: Medulloblastoma- SHH variant Axial T2WI (a) show a hyperintense mass epicentred in the right cerebellar hemisphere showing few hyperintense foci within the tumoral core on T1WI (b). DWI show exuberant diffusion restriction (c) with minimal enhancement on post contrast T1WI (d)

Financial support and sponsorship
Nil.

Conflicts of interest
There are no conflicts of interest.

References

1. Ostrom QT, Gittleman H, Liao P, Vecchione-Koval T, Wolinsky Y, Kruchko C, *et al*. CBTRUS Statistical Report: Primary brain and other central nervous system tumors diagnosed in the United States in 2010–2014. Neuro-Oncol. 2017 Nov 6;19(suppl_5):v1–88.
2. Gillies RJ, Kinahan PE, Hricak H. Radiomics: Images Are More than Pictures, They Are Data. Radiology. 2016 Feb;278(2):563–77.
3. Singh G, Manjila S, Sakla N, True A, Wardeh AH, Beig N, Vaysberg A, Matthews J, Prasanna P, Spektor V. Radiomics and radiogenomics in gliomas: a contemporary update. British journal of cancer. 2021 Aug 31;125(5):641-57.
4. Taha B, Boley D, Sun J, Chen CC. State of radiomics in glioblastoma. Neurosurgery. 2021 Aug 1;89(2):177-84.
5. Liu D, Chen J, Ge H, Yan Z, Luo B, Hu X, Yang K, Liu Y, Liu H, Zhang W. Radiogenomics to characterize the immune-related prognostic signature associated with biological functions in glioblastoma. European Radiology. 2023 Jan;33(1):209-20.
6. Kumar V, Gu Y, Basu S, Berglund A, Eschrich SA, Schabath MB, *et al*. Radiomics: the process and the challenges. Magn Reson Imaging. 2012 Nov;30(9):1234–48.
7. Gulsen S. Achieving Higher Diagnostic Results in Stereotactic Brain Biopsy by Simple and Novel Technique. Open Access Maced J Med Sci. 2015 Mar 15;3(1):99–104.
8. Gillies RJ, Kinahan PE, Hricak H. Radiomics: Images Are More than Pictures, They Are Data. Radiology. 2016 Feb;278(2):563–77.
9. Aerts HJWL, Velazquez ER, Leijenaar RTH, Parmar C, Grossmann P, Carvalho S, *et al*. Decoding tumour phenotype by noninvasive imaging using a quantitative radiomics approach. Nat Commun. 2014 Jun 3; 5:4006.
10. Zhou M, Scott J, Chaudhury B, Hall L, Goldgof D, Yeom KW, *et al*. Radiomics in Brain Tumor: Image Assessment, Quantitative Feature Descriptors, and Machine-Learning Approaches. AJNR Am J Neuroradiol. 2018 Feb;39(2):208–16.
11. Van Lent DI, Van Baarsen KM, Snijders TJ, Robe PAJT. Radiological differences between subtypes of WHO 2016 grade II–III gliomas: a systematic review and meta-analysis. Neuro-Oncol Adv. 2020 Jan 1;2(1):vdaa044.
12. Wu S, Meng J, Yu Q, Li P, Fu S. Radiomics-based machine learning methods for isocitrate dehydrogenase genotype prediction of diffuse gliomas. J Cancer Res Clin Oncol. 2019 Mar;145(3):543–50.
13. Hwan-Ho Cho null, Hyunjin Park null. Classification of low-grade and high-grade glioma using multi-modal image radiomics features. Annu Int Conf IEEE Eng Med Biol Soc IEEE Eng Med Biol Soc Annu Int Conf. 2017 Jul;2017:3081–4.
14. Patel SH, Poisson LM, Brat DJ, Zhou Y, Cooper L, Snuderl M, *et al*. T2–FLAIR Mismatch, an Imaging Biomarker for IDH and 1p/19q Status in Lower-grade Gliomas: A TCGA/TCIA Project. Clin Cancer Res. 2017 Oct 15;23(20):6078–85.
15. Lee MD, Patel SH, Mohan S, Akbari H, Bakas S, Nasrallah MP, *et al*. Association of partial T2-FLAIR mismatch sign and isocitrate dehydrogenase mutation in WHO grade 4 gliomas: results from the ReSPOND consortium. Neuroradiology. 2023 Sep;65(9):1343–52.
16. Goyal A, Yolcu YU, Goyal A, Kerezoudis P, Brown DA, Graffeo CS, *et al*. The T2-FLAIR-mismatch sign as an imaging biomarker for IDH and 1p/19q status in diffuse low-grade gliomas: a systematic review with a Bayesian approach to evaluation of diagnostic test performance. Neurosurg Focus. 2019 Dec 1;47(6):E13.
17. Wang K, Wang Y, Fan X, Wang J, Li G, Ma J, *et al*. Radiological features combined with IDH1 status for predicting the survival outcome of glioblastoma patients. Neuro-Oncol. 2016 Apr;18(4):589–97.
18. Ding H, Huang Y, Li Z, Li S, Chen Q, Xie C, *et al*. Prediction of IDH Status Through MRI Features and Enlightened Reflection on the Delineation of Target Volume in Low-Grade Gliomas. Technol Cancer Res Treat. 2019 Jan 1;18:1533033819877167.
19. Broen MPG, Smits M, Wijnenga MMJ, Dubbink HJ, Anten MHME, Schijns OEMG, *et al*. The T2-FLAIR mismatch sign as an imaging marker for non-enhancing IDH-mutant, 1p/19q-intact lower-grade glioma: a validation study. Neuro-Oncol. 2018 Sep 3;20(10):1393–9.
20. Foltyn M, Nieto Taborda KN, Neuberger U, Brugnara G, Reinhardt A, Stichel D, *et al*. T2/FLAIR-

mismatch sign for noninvasive detection of IDH-mutant 1p/19q non-codeleted gliomas: validity and pathophysiology. Neuro-Oncol Adv. 2020;2(1):vdaa004.

21. Xing Z, Yang X, She D, Lin Y, Zhang Y, Cao D. Noninvasive Assessment of IDH Mutational Status in World Health Organization Grade II and III Astrocytomas Using DWI and DSC-PWI Combined with Conventional MR Imaging. AJNR Am J Neuroradiol. 2017 Jun;38(6):1138–44.
22. Leu K, Ott GA, Lai A, Nghiemphu PL, Pope WB, Yong WH, *et al*. Perfusion and diffusion MRI signatures in histologic and genetic subtypes of WHO grade II-III diffuse gliomas. J Neurooncol. 2017 Aug;134(1):177–88.
23. Zhou H, Chang K, Bai HX, Xiao B, Su C, Bi WL, *et al*. Machine learning reveals multimodal MRI patterns predictive of isocitrate dehydrogenase and 1p/19q status in diffuse low- and high-grade gliomas. J Neurooncol. 2019 Apr;142(2):299–307.
24. Nam YK, Park JE, Park SY, Lee M, Kim M, Nam SJ, *et al*. Reproducible imaging-based prediction of molecular subtype and risk stratification of gliomas across different experience levels using a structured reporting system. Eur Radiol. 2021 Oct;31(10):7374–85.
25. Yamashita K, Togao O, Kikuchi K, Kuga D, Sangatsuda Y, Fujioka Y, *et al*. Cortical high-flow sign on arterial spin labeling: a novel biomarker for IDH-mutation and 1p/19q-codeletion status in diffuse gliomas without intense contrast enhancement. Neuroradiology. 2023 Sep;65(9):1415–8.
26. Jagtap J, Saini J, Santosh V, Ingalhalikar M. Predicting the molecular subtypes in gliomas using T2-Weighted MRI. InProceedings of the 2nd International Conference on Data Engineering and Communication Technology: ICDECT 2017 2019 (pp. 65-73). Springer Singapore.
27. Lu CF, Hsu FT, Hsieh KLC, Kao YCJ, Cheng SJ, Hsu JBK, *et al*. Machine Learning-Based Radiomics for Molecular Subtyping of Gliomas. Clin Cancer Res Off J Am Assoc Cancer Res. 2018 Sep 15;24(18):4429–36.
28. Choi KS, Choi SH, Jeong B. Prediction of IDH genotype in gliomas with dynamic susceptibility contrast perfusion MR imaging using an explainable recurrent neural network. Neuro-Oncol. 2019 Sep 6;21(9):1197–209.
29. Akkus Z, Ali I, Sedlář J, Agrawal JP, Parney IF, Giannini C, *et al*. Predicting Deletion of Chromosomal Arms 1p/19q in Low-Grade Gliomas from MR Images Using Machine Intelligence. J Digit Imaging. 2017 Aug;30(4):469–76.
30. Johnson DR, Giannini C, Vaubel RA, Morris JM, Eckel LJ, Kaufmann TJ, *et al*. A Radiologist's Guide to the 2021 WHO Central Nervous System Tumor Classification: Part I—Key Concepts and the Spectrum of Diffuse Gliomas. Radiology. 2022 Sep;304(3):494–508.
31. Saini J, Gupta RK, Kumar M, Singh A, Saha I, Santosh V, *et al*. Comparative evaluation of cerebral gliomas using rCBV measurements during sequential acquisition of T1-perfusion and T2*-perfusion MRI. Jiang Q, editor. PLOS ONE. 2019 Apr 24;14(4):e0215400.
32. Kickingereder P, Bonekamp D, Nowosielski M, Kratz A, Sill M, Burth S, *et al*. Radiogenomics of Glioblastoma: Machine Learning-based Classification of Molecular Characteristics by Using Multiparametric and Multiregional MR Imaging Features. Radiology. 2016 Dec;281(3):907–18.
33. Li ZC, Bai H, Sun Q, Li Q, Liu L, Zou Y, *et al*. Multiregional radiomics features from multiparametric MRI for prediction of MGMT methylation status in glioblastoma multiforme: A multicentre study. Eur Radiol. 2018 Sep;28(9):3640–50.
34. Korfiatis P, Erickson B. Deep learning can see the unseeable: predicting molecular markers from MRI of brain gliomas. Clin Radiol. 2019 May;74(5):367–73.
35. Rathore S, Akbari H, Bakas S, Pisapia JM, Shukla G, Rudie JD, *et al*. Multivariate Analysis of Preoperative Magnetic Resonance Imaging Reveals Transcriptomic Classification of de novo Glioblastoma Patients. Front Comput Neurosci. 2019;13:81.
36. Macyszyn L, Akbari H, Pisapia JM, Da X, Attiah M, Pigrish V, *et al*. Imaging patterns predict patient survival and molecular subtype in glioblastoma via machine learning techniques. Neuro-Oncol. 2016 Mar;18(3):417–25.
37. Chauhan RS, Kulanthaivelu K, Kathrani N, Kotwal A, Bhat MD, Saini J, *et al*. Prediction of H3K27M mutation status of diffuse midline gliomas using MRI features. J Neuroimaging Off J Am Soc Neuroimaging. 2021 Nov;31(6):1201–10.
38. Kathrani N, Chauhan RS, Kotwal A, Kulanthaivelu K, Bhat MD, Saini J, *et al*. Diffusion and perfusion imaging biomarkers of H3 K27M mutation status in diffuse midline gliomas. Neuroradiology. 2022 Aug;64(8):1519–28.
39. Guo W, She D, Xing Z, Lin X, Wang F, Song Y, *et al*. Multiparametric MRI-Based Radiomics Model for Predicting H3 K27M Mutant Status in Diffuse Midline Glioma: A Comparative Study Across Different Sequences and Machine Learning Techniques. Front Oncol. 2022 Mar 3;12:796583.
40. Puntonet J, Dangouloff-Ros V, Saffroy R, Pagès M, Andreiuolo F, Grill J, *et al*. Historadiological correlations in high-grade glioma with the histone 3.3 G34R mutation. J Neuroradiol. 2018 Sep;45(5):316–22.
41. Tauziède-Espariat A, Debily MA, Castel D, Grill J, Puget S, Roux A, *et al*. The pediatric

supratentorial MYCN-amplified high-grade gliomas methylation class presents the same radiological, histopathological and molecular features as their pontine counterparts. Acta Neuropathol Commun. 2020 Dec;8(1):104.

42. Shakur SF, McGirt MJ, Johnson MW, Burger PC, Ahn E, Carson BS, *et al*. Angiocentric glioma: a case series. J Neurosurg Pediatr. 2009 Mar;3(3):197–202.
43. Chiang J, Harreld JH, Tinkle CL, Moreira DC, Li X, Acharya S, *et al*. A single-center study of the clinicopathologic correlates of gliomas with a MYB or MYBL1 alteration. Acta Neuropathol (Berl). 2019 Dec;138(6):1091–2.
44. Johnson DR, Giannini C, Jenkins RB, Kim DK, Kaufmann TJ. Plenty of calcification: imaging characterization of polymorphous low-grade neuroepithelial tumor of the young. Neuroradiology. 2019 Nov;61:1327-32.
45. Jabeen S, Konar SK, Prasad C, Mahadevan A, Beniwal M, Sadashiva N, *et al*. Conventional and Advanced Magnetic Resonance Imaging Features of Supratentorial Extraventricular Ependymomas. J Comput Assist Tomogr. 2020;44(5):692–8.
46. Mangalore S, Aryan S, Prasad C, Santosh V. Imaging characteristics of supratentorial ependymomas: Study on a large single institutional cohort with histopathological correlation. Asian J Neurosurg. 2015;10(4):276–81.
47. Safai A, Shinde S, Jadhav M, Chougule T, Indoria A, Kumar M, *et al*. Developing a Radiomics Signature for Supratentorial Extra-Ventricular Ependymoma Using Multimodal MR Imaging. Front Neurol. 2021 Jul 22;12:648092.
48. Mata-Mbemba D, Zapotocky M, Laughlin S, Taylor MD, Ramaswamy V, Raybaud C. MRI Characteristics of Primary Tumors and Metastatic Lesions in Molecular Subgroups of Pediatric Medulloblastoma: A Single-Center Study. Am J Neuroradiol. 2018 May;39(5):949–55.
49. Zhang M, Wong SW, Wright JN, Wagner MW, Toescu S, Han M, *et al*. MRI Radiogenomics of Pediatric Medulloblastoma: A Multicenter Study. Radiology. 2022 Aug;304(2):406–16.
50. Dangouloff-Ros V, Tauziède-Espariat A, Roux CJ, Levy R, Grévent D, Brunelle F, *et al*. CT and Multimodal MR Imaging Features of Embryonal Tumors with Multilayered Rosettes in Children. AJNR Am J Neuroradiol. 2019 Apr;40(4):732–6.
51. Theeler BJ, Ellezam B, Sadighi ZS, Mehta V, Tran MD, Adesina AM, *et al*. Adult pilocytic astrocytomas: clinical features and molecular analysis. Neuro-Oncol. 2014 Jun;16(6):841–7.
52. Kerleroux B, Cottier JP, Janot K, Listrat A, Sirinelli D, Morel B. Posterior fossa tumors in children: Radiological tips & tricks in the age of genomic tumor classification and advance MR technology. J Neuroradiol. 2020 Feb;47(1):46–53.

Author Queries???
AQ1: Kindly provide Figures 1 and 9 citations in the text part
AQ3: Kindly check the heading level throughout the article.
AQ5: Kindly mention part label a in the figure caption.